40th Thermophysics Conference
23 - 26 June 2008, Seattle, Washington

AIAA 2008-4250

Numerical Study on Thermal Design for a DLP Projector

Sheam-Chyun Lin[1], Fu-Sheng Chuang[2], Ming-Lun Tsai[3], and Hsien-Chang Shih[3]
National Taiwan University of Science and Technology, Taipei, Taiwan, 106, R.O.C.

Yu-Shan Luo[4] and Yung-Tai Chou[4]
Tungnan University, Taipei County, Taiwan, 222, R.O.C.

Due to its compact size and high-resolution video output, digital light processor (DLP) video projector has become more popular in the current market. However, reducing projector size generates a problem of more heat dissipation being crowded into less space and leads to the need for an effective heat removal mechanism. As a result, this numerical investigation is aimed to examine and enhance the thermal management of a DLP projector. At first, numerical simulation on a DLP projector is performed by using a CFD code. Later, the detailed velocity, pressure, and temperature distributions are visualized numerically and utilized to identify the components in which their temperatures are higher than the thermal-design limitations stated in DLP products thermal design guide. These high-temperature regions include color-wheel motor, cooling fan, and exhaust fan. Furthermore, based on this numerical outcome, several modifications are proposed to improve the flow patterns associated with these ill-design portions. Among them, the appropriate guide plate is added to prevent the airflow circulation within the projector that causes extreme temperatures for components in the affected area. Also, the extra vent area is placed near the inlet region of cooling fan to reduce the system resistance and ensure that the airflow is replaced by the cooler intake air. Thereafter, numerical simulations are executed to validate the corresponding improvements generated by those new alternatives. In conclusion, simulation results show that significant temperature drops (roughly 30~45℃) on color-wheel motor and cooling fans are achieved.

I. Introduction

WITH the rapid development of digital micromirror device (DMD) technology, portable video projectors are becoming more popular in the home entertainment and presentation applications. According to the different optical designs on image formulation, video projectors can be classified into three types-- LCD (liquid crystal display), DLP (digital light processor), and LCOS (liquid crystal on silicon) projectors. In general, LCD projector has the biggest size and heaviest weight among them, so the high-temperature flow induced from the electric components can be exhausted along a smooth flow path throughout the ample space inside an LCD projector. Therefore, maintaining bulb temperature below a certain limit for a long lamp life can be achieved without too much difficulty. However, owing to the mechanisms of reflection, refraction, and dispersion, the light brightness emitted from the high-pressure mercury lamp decays significantly along the optical path, thus the image generated by an LCD projector is not as bright as the other two's.

On the contrary, it is obvious that, after traveling through the color-wheel motor, the window aperture, prism, and DMD, the light emitted from the lamp still can project on the lens without serious illumination loss. Hence, the quality and brightness of the video outputs generated by DLP and LCOS projectors are much better than that of LCD projector. Nevertheless, due to the difficulty in manufacturing LCOS chip, LCOS projector is still a future

[1] Professor, Department of Mechanical Engineering, 43, Sec. 4, Keelung Road, Taipei, Taiwan 106, R.O.C.
[2] Associate Professor, Department of Mech. Engineering, 43, Sec. 4, Keelung Road, Taipei, Taiwan 106, R.O.C.
[3] Graduate Student, Department of Mechanical Engineering, 43, Sec. 4, Keelung Road, Taipei, Taiwan 106, R.O.C.
[4] Assistant Professor, Department of Mech. Engineering, Sec. 3, Beishen Rd., Taipei County, Taiwan 222, R.O.C.

video projector with great potential. Nowadays, the DLP projector is dominant in the market of portable video projectors. Table 1 lists the performance comparison for these three video projectors.

Table 1 Comparison among different projectors

	LCD	DLP	LCOS
Color & resolution	Poor	Better	Better
Brightness	Poor	Better	Better
Thermal cooling	Better	Poor	Better
Lamp life	Better	Poor	Poor
Size	Large	Small	Small

Due to the strong demand in decreasing projector size and weight while increasing brightness, the power density inside a DLP projector increases dramatically. It follows that thermal management becomes more important and challenging with each new generation of projectors. Thus, video projectors use cooling fans to circulate air through their chassis and convectively cool the internal components. If the projector size continuously reduces as expected, the overall system resistance becomes larger and eventually suppresses the convective flow inside it. This fact significantly downgrades the fan performance and the heat removal capability. This trend in projector design leads to a substantial need for understanding thermal and flow fields associated with the entire projector system, which be made of many electric components. In 2000 Wang[1] mentioned that, without taking the flow resistances of components in a system viewpoint into consideration, using multiple fans cannot guarantee to remove the dissipated heat successfully. Later, Turner and Rotron[2] also proposed two important criterions for placing the cooling fan:

1. Fan can't be set too close to exhaled-air outlet for preventing the backflow of discharged exhaust heat.
2. The fan location must be close to the heat-generating components. The heat-removing mechanism would not work if the cool air brought in by the cooling fan can not mix with the hot air in the vicinity of heat source.

In other words, the flow path for air stream is the essential factor for a successful thermal management on electronic devices. Li[3] is the first investigator to carry out the heat dissipation improvement on a commercial DLP Projector. He proposed four thermal solutions by varying the sizes and locations of two cooling fans. By experimental validation, he successfully found an appropriate alternative to secure a smooth flow path and keep all the electronic components operating under their safety temperature limits. Nevertheless, the shortcoming of Li's work is the expensive cost on fabricating prototypes, the time-consuming test, and the try-and-error nature. To fix these deficiencies and provide a logical foundation for design amendment, a reliable flow visualization tool is needed to identify the detailed physical phenomenon inside the DLP projector for setting a proper modification.

Consequently, this numerical investigation is aimed to examine and enhance the thermal management of a DLP projector. At first, numerical simulation on a DLP projector is performed by using a commercial CFD code. This CFD outcome will be compared with the experimental result for establishing its reliability. Later, the detailed velocity, pressure, and temperature distributions are visualized numerically and utilized to identify the components in which their temperatures are higher than the thermal-design limitations stated in DLP products thermal design guide[4]. These high-temperature regions include filter lens, color-wheel motor, cooling fan, and exhaust fan. Furthermore, based on this numerical outcome, several modifications are proposed to improve the flow patterns associated with these ill-design portions. Thereafter, numerical simulations are executed to validate the corresponding improvements generated by those new alternatives.

II. Physical Model and Grid Arrangement

It needs a high luminance bulb to be light source in the interior of DLP projector. Usually, the electric power consumption of bulb is very high, such as 150W or even higher than 200W. This lamp source contains significant waste energy outside the visible spectrum. This dissipated energy can damage the device and other projector components if it is not managed properly. Thus it is the most important issue to solve the heat-dissipating problem in DLP projector. In this study, first of all, the original thermal solution of a typical DLP projector is investigated. The forming mechanism of internal flow circulation and the high temperature region are identified and discussed through carefully checking the numerical outcomes. Thereafter, some modifications are proposed to fix the above shortcomings. The geometry and flow path of the DLP projector are described and the strategy of constructing grid system is explained briefly in this section.

A. Physical Models

Figure 1 schematically illustrates a typical DLP projector. Obviously, the flow field inside it is indeed very complex, and there is no published literature in that area. The original flow field design of DLP Projector in the study uses two axial-flow fans blowing air to enhance the forced convection. As shown in Fig.1, the environmental cool air (25℃) is sucked into the projector through the inlet with the aids of an axial-flow fan placed in projector interior, which is thus named as the inner fan. Then the air passes through DMD's cooling sink, PC boards, and power supply, to produce an approximate 45℃ gas flow at the inlet of inner fan, as a result of the wasted heat generated from the above components. By means of the operation of inner fan, this air flow is discharged to the region between inner fan and bulb for cooling the bulb. When the flow passes via the high-temperature bulb, a hot and stagnant air stream is formed in the space between the bulb front and the color-wheel motor. This high-temperature zone will cause the color-wheel motor and optical filter to work under an unacceptable condition. Hence, an outlet fan is used to offer an extra thrust for driving this hot air to the outlet fan; in sequence, the dissipated energy is expelled out of the projector along with the exhausted hot airstream at the fan discharge.

Since the temperature can reach 330℃ on the bulb surface, which results in a heating effect on the neighboring electronic components. Thus fine grid distribution should be imposed on these noted portions for an accurate numerical simulation. Also, without distorting the practical physical configuration, some simplifications are also applied in establishing the appropriate numerical model. Several important components of DLP projector are illustrated as follows:

(1) Bulb

An ultra high-pressure mercury bulb (Osram120W bulb) is used.

(2) Color-wheel motor

High temperature and noise are produced under the operation of motor, which is actuated by the color-wheel motor. Thus, a rubber spacer is used for fixing color-wheel. Because of shock absorbance of rubber material, it can decrease the noise production.

(3) Optical tube components

There are four pieces of high reflective lenses in a hollow light tube. The lenses shift and focus the bright rays in optical tube, then project on DMD, reflect to lens set for producing images.

(4) DMD with cooling fins

Light illuminates and strikes on lenses and filters of DMD, therefore it produce considerably high heat. Several cooling fins are pasted on the backside of DMD module in order to keep its temperature distribution below the critical temperature limit.

(5) Cooling fan

Owing to the compact size of DLP projector, the inner temperature is higher than that of LCD Projector, so using natural convection for cooling is not sufficient. Two $60 \times 60 \times 20$ mm^3 axial-flow fans with NACA-4412 airfoil blades are used here.

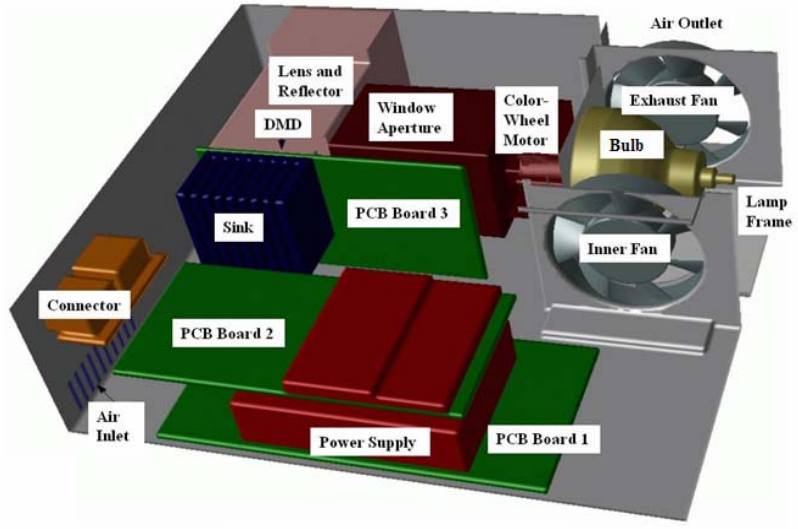

Fig. 1 Sketch of the DLP projector.

B. Model Analysis and Grids Generation

As stated previously, the numerical model is constructed based on the actual specifications of DLP projector and interior electronic components. Also, proper boundary conditions are set according to the practical working environment for solving the thermal/fluid distribution inside this DLP projector. When constructing the numerical model, grids generation must be made in accordance with the flow field and heat distribution of projector interior. The grid system and the detailed distribution for this projector are shown in Fig. 2. Note that fine grids are generated near regions having dramatic variations on flow and temperature distributions. Those portions include the regions near the cooling fans, lamp, color-wheel motor, and DMD module. In order to simulate the infinite ambient environment, an extended calculation domain is constructed to enclose the inlet and outlet of projector (see Fig. 2b). Note that grids refinement is adopted for the severe variation of airflow speed at the inlet and outlet of inner fan. Also the tiny zone between color-wheel motor and bulb need to be handled carefully since the bulb temperature is about 330^{o}C. Therefore, an appropriate grid system is constructed successfully to accurately predict the physical phenomenon in those specific areas.

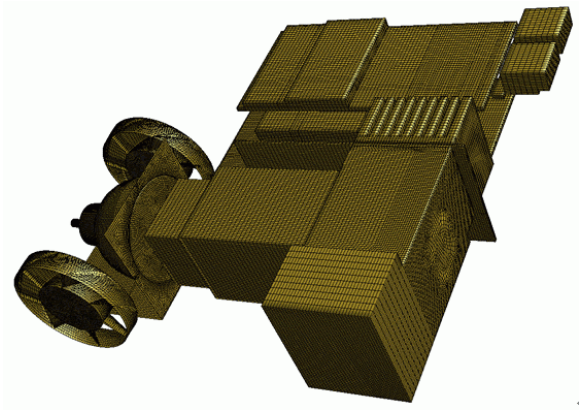

(a) Inner electric components

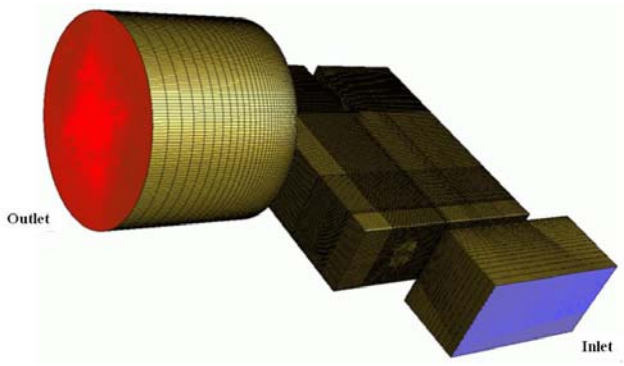

(b) Total grid system

Fig. 2 The grid system for the DLP projector.

When constructing model, grids generation must be made in accordance with the flow field and heat distribution of interior projector. Grid refinement must be done in the region where physical scalar variation is heavier, which means refining grids more detailed in the region of great change in the flow field heat distribution, then reveal the physical phenomenon in post process obviously. In order to present outer flow field at infinity, a more extensive calculation domain is created in inlet and outlet of projector, and outside environment pressure is set P_0. Since the variation in physical phenomenon is not obvious, coarse grids refinement is adopted, because of the severe variation of airflow speed in inner fan inlet and outlet, which is near the bulb with high temperature, so the grids are refined. Also front area of color-wheel motor and bulb is need to be refined, since the bulb temperature is about 300^{o}C, color-wheel motor and bulb are quite close, the grids in the region need to be arranged properly. As to the light

emitted from bulb of fluorescent tube components transmit the inner lens, and project on DMD, then shoot by camera, therefore grids refinement of component where light passes through is executed carefully the when generating mesh (Fig. 2), then obtain the most realistic results, overall outside grids is shown as Fig. 3.

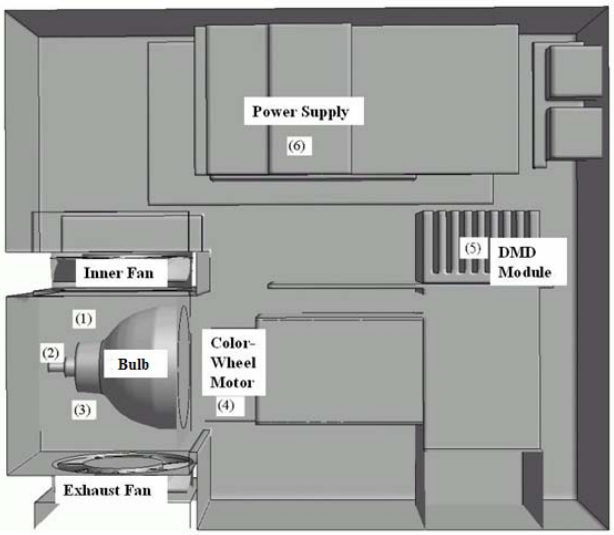

Fig. 3 Six temperature measuring points inside the DLP projector.

III. Numerical Analysis

In order to capture the complex physical features of a DLP projector, the numerical software Fluent[5] is utilized to perform the flow field analysis. Fluent is a commercial CFD code, which solves the Navier-Stokes equation using an unstructured finite-volume-method[6]. The thermal/flow field simulation of a DLP projector is executed by solving a three-dimensional Reynolds-averaged Navier-Stokes equation together with a modified SIMPLE method[7]. The flow chart of the SIMPLE method is plotted in Fig. 3. Besides, the modified $k-\varepsilon$ turbulent model presented by Chen and Kim[8] is applied to evaluate the turbulent diffusivities. This section illustrates the governing equation, numerical scheme, code and grid verifications used in numerical simulation.

A. Governing Equations and Turbulence Models

The following assumptions are made to simulate the flow field inside the DLP video projector

1. Incompressible, Newtonian fluid is assumed due to the low velocity for a typical projector.
2. The influences of radiation heat, flotation terms, and gravitational effect are included.
3. Non-slip boundary condition is utilized.
4. The atmosphere is set as the boundary conditions at both project inlet and exhaust.

Thus, the mass, momentum, and energy equations are written as:

$$\frac{\partial \rho}{\partial t}+\frac{\partial}{\partial x_j}(\rho \bar{u}_j)=0, \tag{1}$$

$$\frac{\partial}{\partial t}(\rho u_j)+\frac{\partial}{\partial x_j}(\rho \bar{u}_j u_i-\tau_{ij})=-\frac{\partial p}{\partial x_i}, \tag{2}$$

$$\frac{\partial}{\partial t}(\rho h)+\frac{\partial}{\partial x_j}(\rho \bar{u}_j h-F_{h,j})=\frac{\partial p}{\partial t}+u_j\frac{\partial p}{\partial x_j}+\tau_{ij}\frac{\partial u_i}{\partial x_j}+s_h \tag{3}$$

where t, u, $\bar{u}$, p, ρ, τ, and h represent time, absolute velocity, relative velocity, pressure, density, stress tensor, and static entropy, respectively. The governing equations also include a rotation function, s, which is a

function involving components of the rotation vector and radius vector. With the aids of Newtonian flow and Stoke's hypothesis, the stress tensor can be expressed as

$$\tau_{ij} = 2\mu s_{ij} \quad \text{and} \quad s_{ij} = \frac{1}{2}\left(\frac{\partial u_i}{\partial x_j} + \frac{\partial u_j}{\partial u_i}\right), \tag{4}$$

where μ is the dynamic fluid viscosity, and s_{ij} is the rate of strain tensor.

In this study, the $k-\varepsilon$ models developed by Yakhot et al.[9] and Chen and Kim[8] are used to calculate the turbulent Reynolds stresses in momentum equation. These models are summarized as:

RNG k-ε model equation

Turbulence energy

$$\begin{aligned}&\frac{1}{\sqrt{g}}\frac{\partial}{\partial t}\left(\sqrt{g}\rho k\right) + \frac{\partial}{\partial x_i}\left(\rho \tilde{u}_j k - \frac{\mu_{eff}}{\sigma_k}\frac{\partial k}{\partial x_j}\right)\\ &= \mu_t\left(P + P_B\right) - \rho\varepsilon - \frac{2}{3}\left(\mu_T \frac{\partial u_i}{\partial x_i} + \rho k\right)\frac{\partial u_i}{\partial x_i},\end{aligned} \tag{5}$$

Turbulence dissipation rate

$$\begin{aligned}&\frac{1}{\sqrt{g}}\frac{\partial}{\partial t}\left(\sqrt{g}\rho\varepsilon\right) + \frac{\partial}{\partial x_j}\left(\rho \tilde{u}_j \varepsilon - \frac{\mu_{eff}}{\sigma_\varepsilon}\frac{\partial \varepsilon}{\partial x_j}\right)\\ &= C_{\varepsilon 1}\frac{\varepsilon}{k}\left[\mu_t\left(P + C_{\varepsilon 3}P_B\right) - \frac{2}{3}\left(\mu_T \frac{\partial u_i}{\partial x_i}\right)\right] - C_{\varepsilon 2}\rho\frac{\varepsilon^2}{k} - C_{\varepsilon 4}\rho\varepsilon\frac{\partial u_i}{\partial x_i} - \frac{C_\mu \eta^3\left(1 - \frac{\eta}{\eta_0}\right)}{1 + \beta\eta^3}\frac{\rho\varepsilon^2}{k},\end{aligned} \tag{6}$$

Chen and Kim's k-ε model equation

Turbulence energy

$$\begin{aligned}&\frac{1}{\sqrt{g}}\frac{\partial}{\partial t}\left(\sqrt{g}\rho k\right) + \frac{\partial}{\partial x_j}\left(\rho \tilde{u}_j k - \frac{\mu_{eff}}{\sigma_k}\frac{\partial k}{\partial x_j}\right)\\ &= \mu_t\left(P + P_B\right) - \rho\varepsilon - \frac{2}{3}\left(\mu_t \frac{\partial u_i}{\partial x_i} + \rho k\right)\frac{\partial u_i}{\partial x_i},\end{aligned} \tag{7}$$

Turbulence dissipation rate

$$\begin{aligned}&\frac{1}{\sqrt{g}}\frac{\partial}{\partial t}\left(\sqrt{g}\rho\varepsilon\right) + \frac{\partial}{\partial x_j}\left(\rho \tilde{u}_j \varepsilon - \frac{\mu_{eff}}{\sigma_\varepsilon}\frac{\partial \varepsilon}{\partial x_j}\right)\\ &= C_{\varepsilon 1}\frac{\varepsilon}{k}\left[\mu_t\left(P + C_{\varepsilon 3}P_B\right) - \frac{2}{3}\left(\mu_T \frac{\partial u_i}{\partial x_i} + \rho k\right)\frac{\partial u_i}{\partial x_i}\right] - C_{\varepsilon 2}\rho\frac{\varepsilon^2}{k} - C_{\varepsilon 4}\rho\varepsilon\frac{\partial u_i}{\partial x_i} + C_{\varepsilon 5}\mu_t\frac{P^2}{k},\end{aligned} \tag{8}$$

where μ_t is the turbulent viscosity. $C_{\varepsilon 1}$, $C_{\varepsilon 2}$, $C_{\varepsilon 3}$ and $C_{\varepsilon 4}$ are empirical coefficients.

B. Code and Grid Verifications

In order to validate this numerical code and outcome, the comparison between experimental and CFD results is demonstrated here. These calculations include both the determination of grid number and the code validation by comparing with the measuring temperatures at six major heat-producing points, as indicated in Fig. 4.

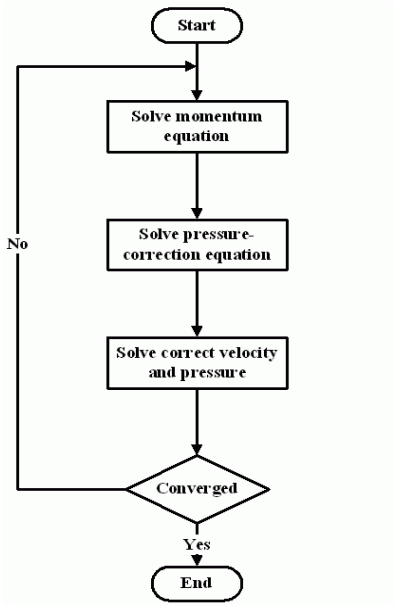

Fig. 4 Flow chart of the SIMPLE scheme.

Four grid systems are considered in a grid number test for this DLP projector to find an appropriate grid number. As listed in Table 2, the computed temperatures of the 2.3 millions grids yield the most accurate result. Obviously, the computational results show a good agreement with experimental results. However, there is only 2% deviation between the CFD outcomes generated from 2.3-million and 2.1-million grid systems. Both grid systems are sufficient to yield the flow characteristics. For reducing the calculation time, the 2,100,000-grid is thus utilized in this numerical study.

Table 2 Computed temperatures for various grid systems

	Measuring Temp (℃)	1.7 Millions	1.9 Millions	2.1 Millions	2.3 Millions
Pt 1	138	158	151	143	142
Pt 2	95	121	113	106	103
Pt 3	148	167	160	156	154
Pt 4	98	120	115	106	104
Pt 5	35	50	46	40	38
Pt 6	46	57	54	51	48

IV. Numerical Results and Discussions of the Original Projector

Here, numerical results are used to visualize and analyze the detailed velocity, pressure, and temperature distributions associated with this DLP projector. It is found that lamp, filter lens, color-wheel motor, cooling fans, optical tube component, and DMD panel are the heated parts, in which their temperatures are higher than the thermal-design limitations stated in DLP products thermal design guide. Consequently, if the temperature of filter lens exceeds the safe range, it will produce ultraviolet (UV) rays, which will shorten the life of electric components downstream; if the color-wheel motor overheats, it will influence the electric circuit system. Thus, it is essential to check the flow patterns near these components carefully for inspiring the probable improving method. The flow pattern descriptions on these heated regions are stated below in details.

A. The Vicinity of Bulb

By carefully checking the calculated results (see Fig. 5), it is found that high temperatures occur in the vicinity of fans, bulbs, light wheel, optical tube as expected. Clearly, surface temperature on the fan hub can reach 102 ^{o}C, which is well beyond the safe operation temperature (70^{o}C) as listed on DLP products thermal design guide of Texas

instrument. Also, a large circulation is observed between the inner fan outlet and bulb due to the inequality distance between them. The discharged air will strike the bulb surface directly after traveling a short distance, which varies along the curved bulb surface. It follows that the flow direction also changes and forms a large vortices between the region confined by bulb and inner fan. Owing to that big vortices, air stream flows slowly with a velocity ranging from 0.1 to 0.3 m/s along the hub surface of inner fan outlet. Certainly, the convective heat transfer is not sufficient to carry the dissipated heat out of projector smoothly.

Besides, there exists an extremely high temperature region, which is close to the inlet side of outlet fan. A high temperature (ranging from 90°C to 93°C) is observed on the exhaust fan hub near the bottom plane of projector. By comparing the temperature and velocity distributions, it is concluded that there is no air blowing to bulbs directly to remove heat in this high temperature zone; hence, the heat-removing effect downgrades and only counts on the operation of the exhaust fan. In sequence, it implies that the waste heat produced from bulb can not be removed out of the projector promptly.

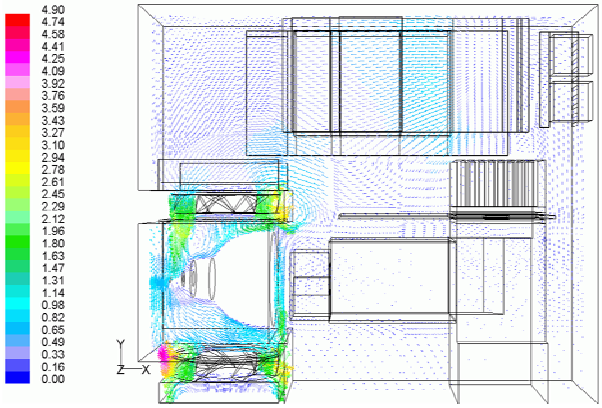

(a) Velocity distribution ($^{m}/_{s}$)

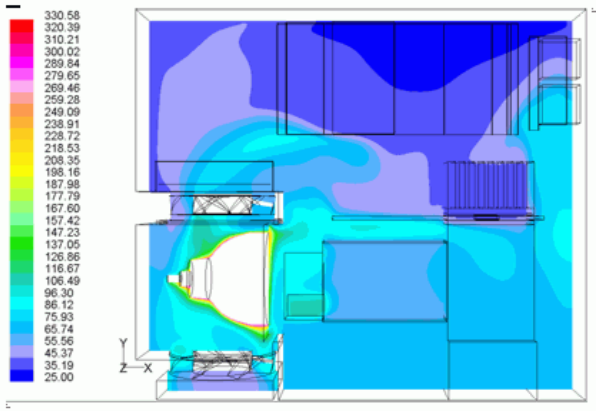

(b) Temperature distribution (℃)

Fig. 5 Calculated results for the original DLP projector.

B. The Vicinity of Inner Fan

Figure 6 plots the velocity and temperature distributions around the vicinity of inner fan. It is found that partial air discharged from outlet side of the inner fan is sucked back to the inlet side and forms a strong circulation (Fig. 6a). This phenomenon is induced by the considerable pressure difference between the high-pressure discharge flow and the low pressure zone (about –5 Pascal) at inner fan inlet. Naturally, the tendency of nearby flow field is moving toward the low-pressure zone; therefore this allows the discharge flow of inner fan to be induced back to its inlet side and form an extensive circulation flow.

Moreover, the hot air generated from the region between bulb and color-wheel motor, is induced to the projector interior and the inner fan inlet (see Fig. 6a); hence it causes that the airflow temperature increases in the vicinity of inner fan as shown in Fig. 6b. This flow pattern has a negative influence on the heat-removing capability for projector. Owing to the raise of inner temperature in projector, it reduces reliability and life of interior components. Thus, if the flow direction at fan outlet can be amended to avoid the circulation, then the hot air in the bulb front might be expelled out of the projector smoothly.

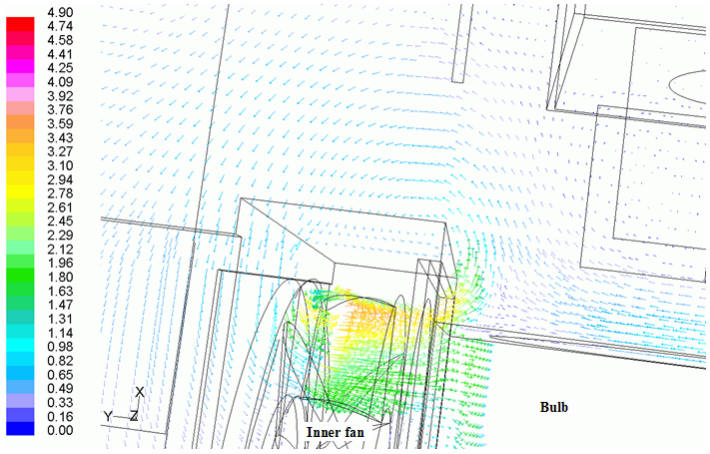

(a) Velocity distribution ($^{m}/_{s}$)

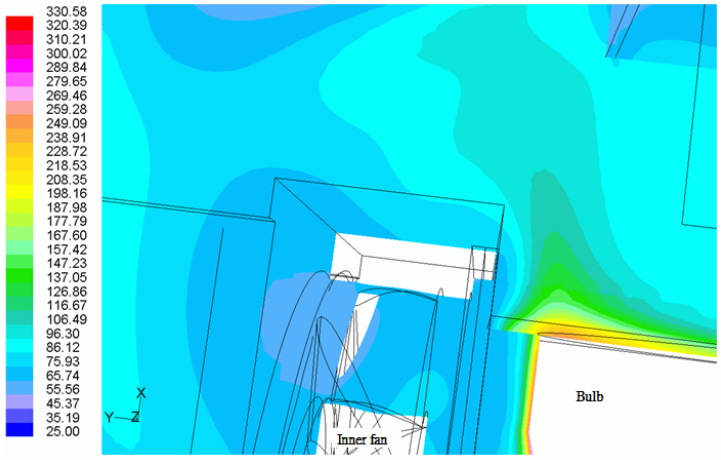

(b) Temperature distribution (℃)

Fig. 6 Enlarged velocity and temperature distributions near the inner fan.

C. Flow Field between Bulb and Color-Wheel Motor

Since the inlet static-pressure of the exhausting fan is higher than that of bulb front region, the hot air in the bulb front cannot discharge to outside environment through the exhauster, smoothly it flows reversely back to the projector interior (see Fig. 7a); therefore the hot air cannot be expelled away by utilizing the exhausting fan. One part of hot air flows to the circulation zone around the inner fan, the other flows to the PCB. Because the air contains high temperature gas, so it forms high temperature region in front of PCB, then affects the reliability and life of electric components.

Moreover, the static pressure distribution maintains at about –5 Pascal in the vicinity of bulb and color-wheel motor, there is no large pressure difference, so it implies the circulation in the vicinity of color-wheel motor, which is produced by the air circulation on bulb front side. Also, as indicated in Fig. 7b, it causes that the air temperature

reaches 93°C in the vicinity of color-wheel motor. If the vortex structure can be destroyed, and air can be induced to fan inlet side, the stability and performance of color-wheel motor can be improved.

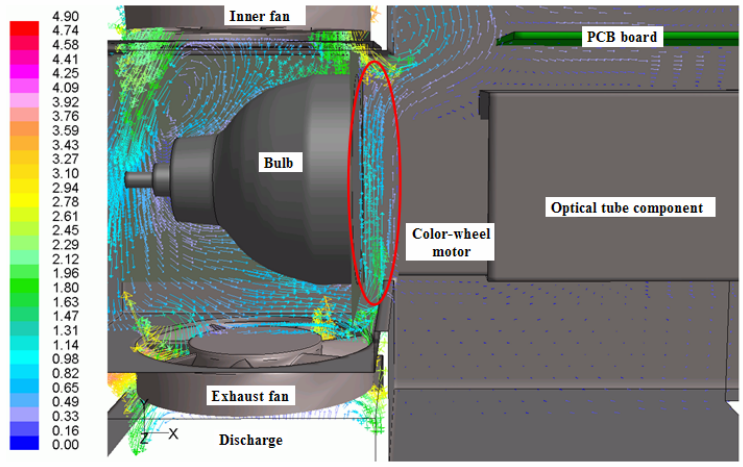

(a) Velocity distribution ($^{m}/_{s}$)

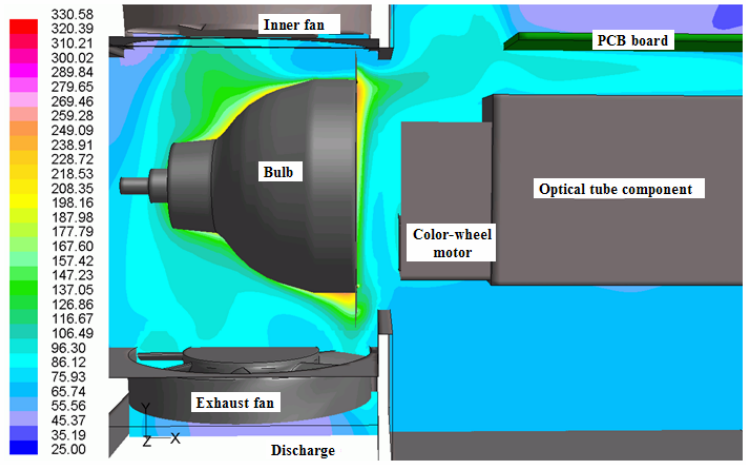

(b) Temperature distribution (℃)

Fig. 7 Calculated results around the vicinity of bulb front.

D. The Bottom Cross-Section of Projector

As stated in previous section, the electric components inside the compact projector considerably retard the airflow path. Part of the high-temperature airflow, originated from the region between bulbs and color-wheel motor, moves to the inlet of inner fan. Consequently, as indicated in Fig. 8a, a hot air flows toward projector base plane is induced by the combined interaction between the inner circulation airflow and the inner fan operation. It stimulates that heated air is restrained in the bottom portion and cannot be ejected out the projector; therefore the bottom temperature distribution increases obviously as illustrated in Fig. 8b.

Additionally, since the air inlet location is lower, the environmental cool air is sucked into the projector and the fluid presents low pressure in the inlet; hence it drives flow motion in the bottom plane. The air stream path is initiated from bulb front side to the PCB and finally to the air inlet (as the cursor indicated direction in Fig. 8a). Because the hot gas generated from bulb front and color-wheel motor flows with this stream, and thus causes the surface temperature of electric components to increase along the airflow path. The maximum temperature even exceeds 90°C (see Fig. 8b), this may result in the low efficiency and a curtailed life.

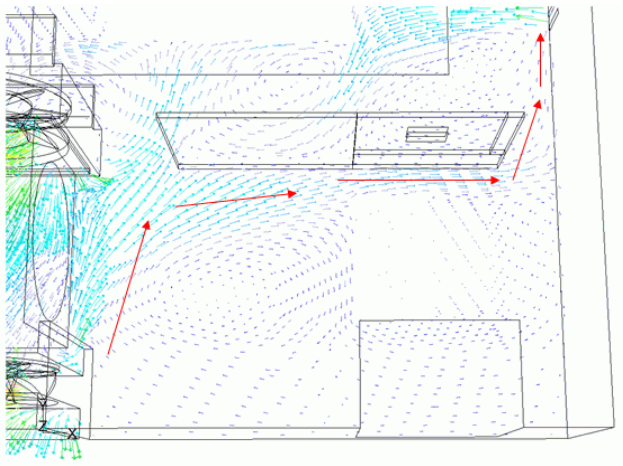

(a) Path and direction of the circulated flow

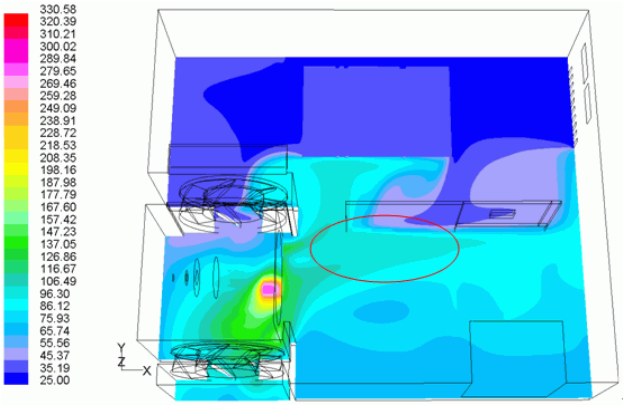

(b) Temperature distribution (℃)

Fig. 8 Calculated results on the bottom cross-section for the original DLP projector.

V. Modification Alternatives

This section is aimed to provide some improving strategies for designing the heat dissipation system for a DLP projector. After carefully checking the numerical results on the velocity and temperature distribution, the drawbacks of the original design are summarized as follows.

(1) The interaction between inner fan and stagnant flow around the bulb front generates flow recirculation, which causes high temperature air not being easy to flow out. The temperatures inside the projector are thus very high.

(2) High temperature air produced by bulb and color-wheel motor flows toward the inside of projector, causing the electronic parts overheated.

(3) High temperature air stays at the bottom plane of projector, resulting in high temperature at the bottom portion of projector.

Furthermore, based on this numerical outcome, several modifications are proposed to improve the flow patterns associated with these ill-design portions. Among them, the appropriate guide plate is added to prevent the airflow circulation within the projector that causes extreme temperatures for components in the affected area. Also, the extra vent area is placed near the inlet region of cooling fan to reduce the system resistance and ensure that the airflow is replaced by the cooler intake air. Thereafter, numerical simulations are executed to validate the corresponding improvements generated by those new alternatives. Summary of the results for the proposed improving strategies are described and evaluated in the following subsections.

A. Installing Guiding Plates

To prevent the flow circulation around the inner fan, guiding plates are proposed to place inside the projector as shown in Fig. 9. Obviously, the circulated air stream, which exits from the inner fan and is sucked back into the

fan's inlet in the original design, can now flow out smoothly as plotted in Fig. 10a. Consequently, the flow path of air is changed after installing the guiding plate; then the hot air can flow efficiently to the outer fan and be blown out of the projector.

Regards the hot air in the bulb front, the guiding plate effectively blocks this air stream, which originally flows toward the inner portion of projector, and guides it to the outer fan direction. It follows that heat produced by the bulb can easily be transported out of the projector and temperatures of the electronic parts around the bulb are lowered considerably.

Additionally, a confined and smooth flow path is formed with the aids of this blocking effect; thus cold ambient air can flow more smoothly to the inlet of the inner fan. Also, temperatures of power supply, DMD module, optical components, and filter lens can be controlled under the safety temperature limit more easily. Apparently, Fig. 10b demonstrates that the installment of guiding plates effectively lowers the temperature of the electronic parts and increases its lifetime.

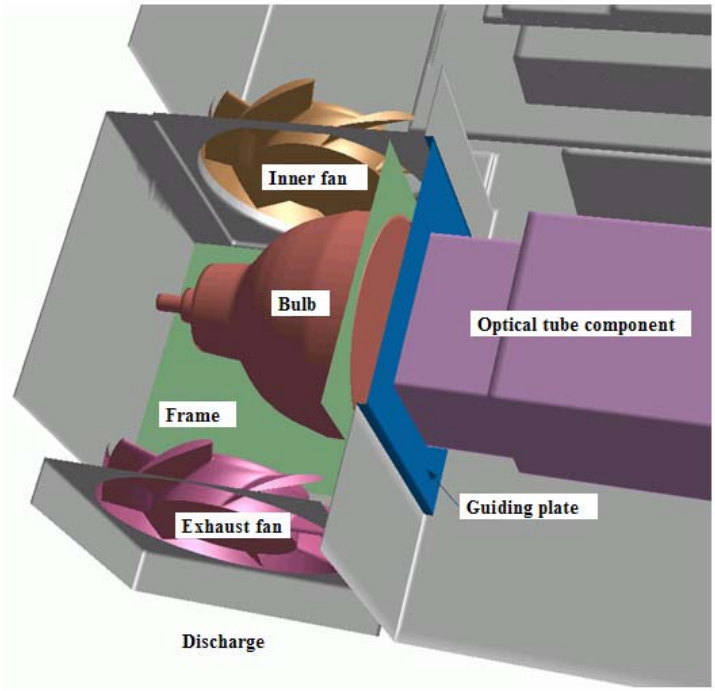

Fig. 9 Schematics of the location for guiding plate.

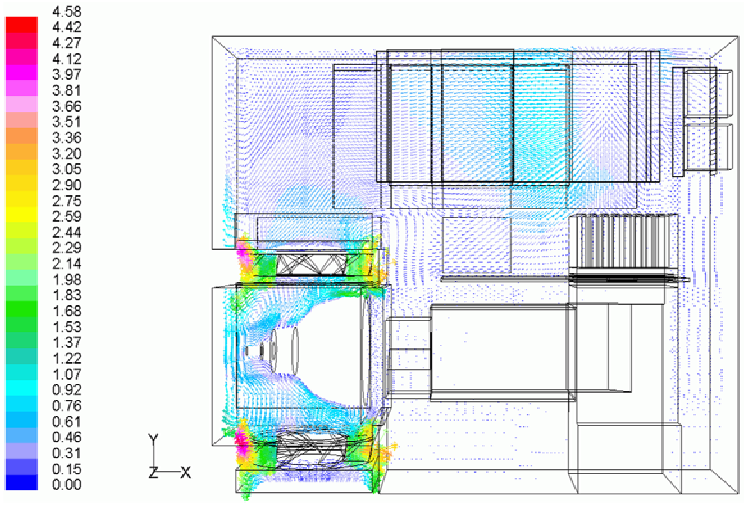

(a) Velocity distribution ($^{m}/_{s}$)

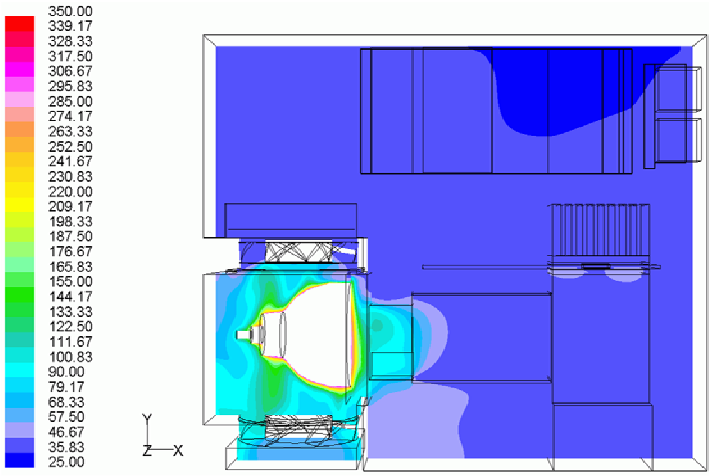

(b) Temperature distribution (℃)

Fig 10 Calculated results for the projector with guiding plate.

B. Increasing Extra Ventilation Openings

As pointed out in previous section, an approximate 20°C temperature increase on the incoming air is observed at the inner fan inlet compared to the ambient temperature. This heating effect on the incoming flow results from the waste heats received along the flow path from projector inlet to the inner fan. In sequence, the cooling effects on the bulb and color wheel motor downgrade extensively. To avoid this deficiency, as indicated in Fig. 11, an extra vent opening is placed near the inlet region of cooling fan to reduce the system resistance and ensure that the incoming airflow is replaced by the cooler intake air. Certainly, air stream exiting the inner fan can flow more collectively and smoothly as indicated in Fig. 12a. Also, temperature at the fan hub is lowered more quickly (see Fig. 12b). Temperature at the surface of color-wheel motor is at 82°C, which is lower than that of the original design and under the 85°C safety limit. Therefore, the steadiness of the projector operation is greatly improved.

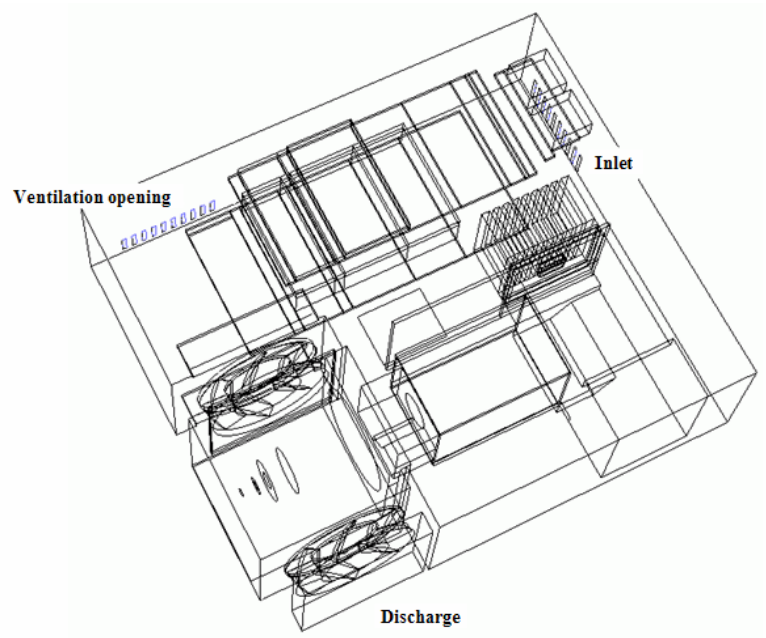

Fig. 11 Schematics of the extra ventilation area.

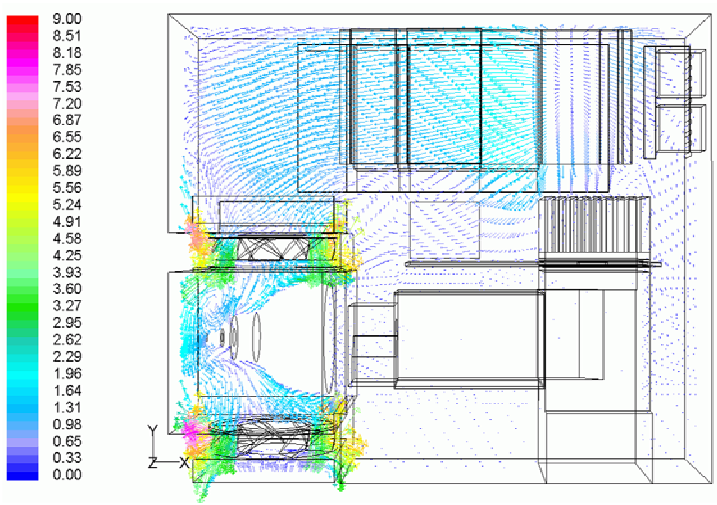

(a)Velocity distribution ($^{m}/_{s}$)

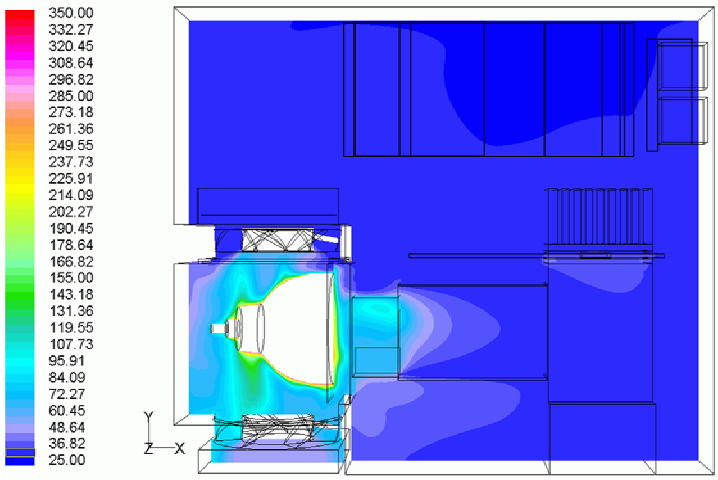

(b) Temperature distribution (℃)

Fig. 12 Calculated results for the DLP projector with an extra ventilation opening.

VI. Concluding Remarks

This numerical investigation intends to examine and enhance the thermal management of a DLP projector. At first, numerical simulation on a DLP projector is performed to visualize the detailed velocity, pressure, and temperature distributions for identifying the high-temperature components, which include the filter lens, color-wheel motor, and cooling fans. The measuring temperature at these hot spots is utilized to validate the CFD model. A good agreement between testing and simulation results is illustrated clearly. After carefully checking the numerical results, the drawbacks of the original design are summarized and analyzed in details.

Moreover, based on these numerical outcomes, two modifications are enforced to improve the flow patterns associated with these ill-design portions. Among them, the appropriate guide plate is added to prevent the airflow circulation within the projector that causes extreme temperatures for components in the affected area. Also, extra open vent area is placed near the inlet region of cooling fan to ensure that the incoming airflow is replaced by the cooler intake air. Thereafter, numerical simulations are executed to validate the corresponding improvements generated by those new alternatives. In conclusion, simulation results show that significant temperature drops (roughly 30~45℃) on color-wheel motor and cooling fans are achieved.

Acknowledgments

The authors would like to thank the National Science Council for financial support of this research under contract No. NSC 95-2625-Z-011-003.

References

[1] Wang, D. G., "Optimization of System Fan Placement," Proceeding of the 2000 IEMT/IMC Thermal Management, April, 2000.

[2] Turner, M. and Rotron, C., "All You Need to Know about Fans," Electronics Cooling, January, 2000. (Also available in http://www.electronics-cooling.com/articles/1996/may/may96_01.php)

[3] Li, J. H., "Introduction of LCD Projector Development and Research on DLP Projector Optical Engine," Master Thesis, Mechanical Engineering Dept., National Chiao-Tung Univ., 2003.

[4] DLPA005, "DLP Products Thermal-Design Guide," Texas Instruments, June 2001.

[5] Fluent 6.1 User's Guide, Fluent Inc., 2004.

[6] Launder, B. E. and Spalding, D. B., "Lectures in Mathematical Models of Turbulence," Academic Press, London, England, 1972.

[7] Patankar, S. V. and Spalding, D. B., "A Calculation Procedure for Heat Mass and Momentum Transfer in Three-Dimensional Parabolic Flows," International Journal of Heat and Mass Transfer, Vol. 15, pp 1787-1806, 1972.

[8] Chen, Y. S. and Kim, S.W., "Computation of Turbulence Flows Using an Extend k-ε Turbulence Closure Model," NASA CR-179204, 1987.

[9] Yakhot, V., Orszag, S. A., Thangam, S., Gatski, T. B., and Speziale, C. G., "Development of Turbulence Models for Shear Flows by a Double Expansion Technique," Physical Fluids, A4, No. 7, pp. 1510-1520, 1992